
Improving Variational Autoencoders with Density Gap-based Regularization

Jianfei Zhang^{1,2} Jun Bai^{1,2} Chenghua Lin³ Yanmeng Wang⁴ Wenge Rong^{1,2}

¹State Key Laboratory of Software Development Environment, Beihang University, China

²School of Computer Science and Engineering, Beihang University, China

³Department of Computer Science, University of Sheffield, United Kingdom

⁴Ping An Technology, China

{zhangjf, ba1_jun, w.rong}@buaa.edu.cn

c.lin@sheffield.ac.uk, wangyanmeng219@pingan.com.cn

Abstract

Variational autoencoders (VAEs) are one of the most powerful unsupervised learning frameworks in NLP for latent representation learning and latent-directed generation. The classic optimization goal of VAEs is to maximize the Evidence Lower Bound (ELBo), which consists of a conditional likelihood for generation and a negative Kullback-Leibler (KL) divergence for regularization. In practice, optimizing ELBo often leads the posterior distribution of all samples converging to the same degenerated local optimum, namely *posterior collapse* or *KL vanishing*. There are effective ways proposed to prevent posterior collapse in VAEs, but we observe that they in essence make trade-offs between posterior collapse and the *hole problem*, i.e., the mismatch between the aggregated posterior distribution and the prior distribution. To this end, we introduce new training objectives to tackle both problems through a novel regularization based on the probabilistic *density gap* between the aggregated posterior distribution and the prior distribution. Through experiments on language modeling, latent space visualization, and interpolation, we show that our proposed method can solve both problems effectively and thus outperforms the existing methods in latent-directed generation. To the best of our knowledge, we are the first to jointly solve the hole problem and posterior collapse.

1 Introduction

As one of the most powerful likelihood-based generative models, variational autoencoders (VAEs) [21, 32] are designed for probabilistic modeling directed by continuous latent variables, which are successfully applied in many NLP tasks, e.g., dialogue generation [45, 14], machine translation [34, 12], recommendation [10], and data augmentation [43, 39]. One of the major advantages of VAEs is the flexible latent representation space, which enables easy manipulation of high-level semantics on corresponding representations, e.g., guided sentence generation with interpretable vector operators.

Despite the attractive theoretical strengths, VAEs are observed to suffer from a well-known problem named *posterior collapse* or *KL vanishing* [21, 24], an optimum state of VAEs when the posterior distribution contains little information about the corresponding datapoint, which is particularly obvious when strong auto-regressive decoders are implemented [46, 4].

Another challenge for VAEs is the *hole problem*, the state when the aggregated (approximate) posterior fails to fit the prior distribution, and thus the inference from the prior distribution becomes no longer suitable to describe the global data distribution [33], which can lead to poor generation quality in VAEs [1, 25].

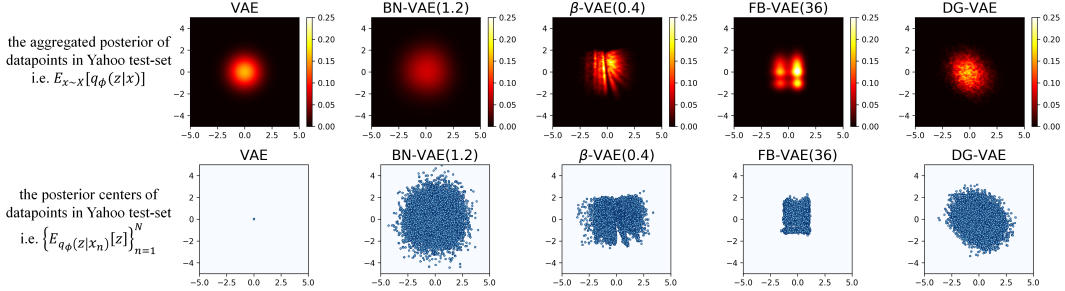


Figure 1: The visualization of the aggregated posterior distributions (the first line) and the posterior centers distributions (the second line) for models on the Yahoo test-set. The vanilla VAEs suffer from *posterior collapse*, i.e., the posterior centers collapse to the same position. Meanwhile, BN-VAEs [46], β -VAEs [18] and FB-VAEs [20] can solve posterior collapse effectively at the cost of bringing the *hole problem*, i.e., mismatch between the aggregated posterior and the prior. Our proposed DG-VAE intends to solve both problems through a novel regularization based on the *density gap*. Illustrations for more datasets, more models, and more dimensions, are shown in Appendix G.

In this work, we perform systematic experiments on VAEs for text generation to study *posterior collapse* and the *hole problem* in existing methods. We demonstrate that VAEs with specific network structures [9, 45] or modified training strategies [6, 13] have limited effect on solving posterior collapse, while VAEs with hard restrictions [8, 41, 46] or weakened KL regularization [18, 20] on the posterior distribution can solve posterior collapse effectively at the expense of the hole problem, as illustrated in Figure 1.

On that basis, we hypothesize that these two problems stem from the conflict between the KL regularization in ELBo and the function definition of the prior distribution. As such, we propose a novel regularization to substitute the KL regularization in ELBo for VAEs, which is based on the *density gap* between the aggregated posterior distribution and the prior distribution. We provide theoretical proof that our method in essence maximizes the ELBo as well as the mutual information between the input and the latent variable.

In terms of Gaussian distribution-based VAEs, we further propose the corresponding marginal regularization on each dimension respectively, and we prove it in essence maximizes the ELBo as well as the sum of mutual information between the input and the latent variable on all dimensions.

To validate our methods in practice, we take experiments on language modeling, latent-guided generation and latent space visualization. We demonstrate that our methods form latent spaces that are both active and consistent with the prior, and thus generate smoother sentences from latent interpolation. The code and data are available at <https://github.com/zhangjif-nlp/DG-VAEs>.

2 Background and Related Work

2.1 VAEs and ELBo

VAEs are proposed to perform efficient inference and learning in directed probabilistic models [21], where the random generation process consists of two steps: (1) sample a latent value \mathbf{z} from the prior $p_{\theta}(\mathbf{z})$; (2) generate a datapoint \mathbf{x} from the conditional distribution $p_{\theta}(\mathbf{x}|\mathbf{z})$. As the true posterior $p_{\theta}(\mathbf{z}|\mathbf{x})$ is intractable, a recognition model $q_{\phi}(\mathbf{z}|\mathbf{x})$ is introduced to approximate the true posterior [21].

Specifically, VAEs represent an observation \mathbf{x} as a latent distribution $q_{\phi}(\mathbf{z}|\mathbf{x})$, from which latent variables are sampled to direct the reconstruction of \mathbf{x} . As the optimization goal of VAEs, the Evidence Lower Bound (ELBo) is composed of a Kullback-Leibler (KL) divergence for regularization on the posterior and a log likelihood for reconstruction conditioned on posterior. The ELBo in fact forms a lower bound on the marginal likelihood given prior latent variables [21], as illustrated in Eq. 1.

$$\begin{aligned} \mathcal{L}_{ELBo}(\theta, \phi; \mathbf{x}) &= \mathbb{E}_{q_{\phi}(\mathbf{z}|\mathbf{x})}[\log p_{\theta}(\mathbf{x}|\mathbf{z})] - D_{KL}(q_{\phi}(\mathbf{z}|\mathbf{x})||p_{\theta}(\mathbf{z})) \\ &\leq \log p_{\theta}(\mathbf{x}) = \log \int p_{\theta}(\mathbf{x}|\mathbf{z})p_{\theta}(\mathbf{z})d\mathbf{z} \end{aligned} \quad (1)$$

2.2 Posterior Collapse

Intuitively, the KL divergence in ELBo (i.e., $D_{KL}(q_\phi(\mathbf{z}|\mathbf{x})||p_\theta(\mathbf{z}))$) encourages the approximate posterior distribution of every single datapoint to be close to the prior [21]. This intends to ensure the prior distribution can depict the latent variable distribution over the data distribution, but it can also lead to posterior collapse when $D_{KL}(q_\phi(\mathbf{z}|\mathbf{x})||p_\theta(\mathbf{z}))$ has much stronger force on $q_\phi(\mathbf{z}|\mathbf{x})$ than $\mathbb{E}_{q_\phi(\mathbf{z}|\mathbf{x})}[\log p_\theta(\mathbf{x}|\mathbf{z})]$ does, which leads that $q_\phi(\mathbf{z}|x) \approx p_\theta(\mathbf{z})\forall x$. In such condition, the sampled latent variable, $\mathbf{z} \sim q_\phi(\mathbf{z}|x)$, contains much more noise than useful information about x [27], and thus the decoder $p_\theta(\mathbf{x}|\mathbf{z})$ becomes insensitive to \mathbf{z} [46].

Early works to solve posterior collapse attribute it to the difficulty in optimizing ELBo, so their methods mainly focus on the training strategies [6, 13, 23]. Some works put emphasis on the semantic learning of the latent variable through specific model structures [9, 45, 29, 17]. Instead of a Gaussian distribution, vMF-VAE [8, 41] adopts the von Mises-Fisher distribution for latent variables, which restricts the posterior latent to a hyperspherical space and forms a constant KL divergence. BN-VAE [46] restricts the posterior distribution through a batch normalization layer with a fixed scale γ , so as to guarantee a positive lower bound of the KL divergence. β -VAE [18] directly changes the weight (denoted as β) of the KL term inside ELBo, while free-bits [20] changes the KL term inside ELBo to a hinge loss term.

In contrast, we hypothesize posterior collapse is due to the conflict between the KL regularization in ELBo and the function definition of the prior distribution, and tackle it through replacing the KL regularization in ELBo with a novel regularization on the aggregated posterior distribution.

2.3 Hole Problem

The *aggregated (approximate) posterior* $q_\phi(\mathbf{z})$ refers to the expectation of the approximate posterior distribution on the data distribution, as defined in Eq. 2, where the distribution of observation \mathbf{x} is represented by the discrete distribution of datapoints in the dataset, i.e., $X = \{x_n\}_{n=1}^N$, $q_\phi(\mathbf{n}) \equiv \frac{1}{N}$, in practice.

$$q_\phi(\mathbf{z}) = \mathbb{E}_{\mathbf{x}}(q_\phi(\mathbf{z}|\mathbf{x})) = \frac{1}{N} \sum_{n=1}^N q_\phi(\mathbf{z}|x_n) \quad (2)$$

Formally, the hole problem refers to the phenomenon that the aggregated posterior distribution $q_\phi(\mathbf{z})$ fails to fit the prior distribution $p_\theta(\mathbf{z})$. Inferences located in the holes (i.e., areas with mismatch between density in $q_\phi(\mathbf{z})$ and $p_\theta(\mathbf{z})$) are observed to generate images that are obscure and corrupted [1], or sentences with incorrect syntax and abnormal semantics [25].

The hole problem of VAEs for image generation is observed in several studies, commonly ascribed to the limited expressivity of the prior distribution and tackled by increasing the flexibility of the prior distribution via hierarchical priors [22], auto-regressive models [16], a mixture of encoders [37], normalizing flows [40], resampled priors [3], and energy-based models [1]. In contrast, we observe that the vanilla VAEs (with standard prior distributions) for text generation have no hole problem, but it arises when existing methods are applied to solve posterior collapse. Therefore, our work is targeted at solving posterior collapse and avoiding the hole problem at the same time, for VAEs with standard prior distributions.

2.4 Regularization on Aggregated Posterior

As the approximate posterior distribution is introduced to approximate the true posterior, i.e., $q_\phi(\mathbf{z}|\mathbf{x}) \approx p_\theta(\mathbf{z}|\mathbf{x})$, the aggregated posterior should be close to the prior as a result, i.e., $q_\phi(\mathbf{z}) \approx p_\theta(\mathbf{z})$. From this point of view, several works are proposed to replace KL regularization (on the posterior distribution of each datapoint separately) in ELBo with a regularization on the aggregated posterior distribution, which can be summarized as Eq. 3, where D is the divergence (or discrepancy) between two distributions.

$$\mathcal{L}_D(\theta, \phi; \mathbf{x}) = \mathbb{E}_{q_\phi(\mathbf{z}|\mathbf{x})}[\log p_\theta(\mathbf{x}|\mathbf{z})] - D(q_\phi(\mathbf{z})||p_\theta(\mathbf{z})) \quad (3)$$

Among them, Adversarial Auto-Encoder (AAE) [28] adopts the Generative Adversarial Network (GAN) [15] framework to regularize the aggregated posterior distribution through Jensen–Shannon

divergence D_{JS} ; Wasserstein Auto-Encoder (WAE) [36, 2] regularizes the aggregated posterior distribution through minimizing Maximum Mean Discrepancy (MMD); Implicit VAE with Mutual Information regularization (iVAE_{MI}) regularizes the aggregated posterior through a dual form of KL divergence D_{KL} on the basis of Implicit VAE (iVAE) [11]. These methods have the same weakness that their approximations of the divergence between two continuous distributions are depicted by merely sampling sets from the distributions, which involves noise from random sampling and can hardly be zero, even for the same distributions.

In contrast, our method approximates the divergence between two continuous distributions in the perspective of their mismatch in PDFs, which we quantify through the *density gap* that can be zero if and only if they are the same, which we describe in section 3.

We validate our method against the aforementioned methods through experiments on a synthetic dataset, the details and results of which are presented in Appendix A.

3 Methodology

Density Gap-based Discrepancy One of the straight manifestations of *holes* in latent space is the mismatch of probabilistic density between $q_\phi(\mathbf{z})$ and $p_\theta(\mathbf{z})$. We quantify this mismatch at a specific position z in the latent space through $DG(\boldsymbol{\theta}, \phi; z)$, which we refer to as *Density Gap*. Here we only consider $z \in \{z | q_\phi(z) > 0\}$.¹ We assume $q_\phi(z)$ and $p_\theta(z)$ are differentiable and $p_\theta(z) > 0$.

$$DG(\boldsymbol{\theta}, \phi; z) = \log \frac{q_\phi(z)}{p_\theta(z)} = \log \frac{\frac{1}{N} \sum_{n=1}^N q_\phi(z|x_n)}{p_\theta(z)} \quad (4)$$

It can be inferred that the expectation of $DG(\boldsymbol{\theta}, \phi; z)$ on $q_\phi(\mathbf{z})$ equals to the KL divergence between $q_\phi(\mathbf{z})$ and $p_\theta(\mathbf{z})$, as illustrated in Eq. 5, which is a strict divergence, i.e., $\mathbb{E}_{z \sim q_\phi(\mathbf{z})}[DG(\boldsymbol{\theta}, \phi; z)] = 0$ iff $q_\phi(\mathbf{z}) = p_\theta(\mathbf{z})$.

$$\mathbb{E}_{z \sim q_\phi(\mathbf{z})}[DG(\boldsymbol{\theta}, \phi; z)] = \mathbb{E}_{z \sim q_\phi(\mathbf{z})}[\log \frac{q_\phi(z)}{p_\theta(z)}] = D_{KL}(q_\phi(\mathbf{z}) \| p_\theta(\mathbf{z})) \geq 0 \quad (5)$$

So, we can approximate and optimize $D_{KL}(q_\phi(\mathbf{z}) \| p_\theta(\mathbf{z}))$ via Monte Carlo, as illustrated in Eq. 6, where $z_s \stackrel{iid}{\sim} q_\phi(\mathbf{z})$ denotes the s^{th} random sample from the aggregated posterior distribution.

$$D_{KL}(q_\phi(\mathbf{z}) \| p_\theta(\mathbf{z})) \approx \frac{1}{S} \sum_{s=1}^S DG(\boldsymbol{\theta}, \phi; z_s) \quad (6)$$

It should be noted that $D_{KL}(q_\phi(\mathbf{z}) \| p_\theta(\mathbf{z}))$ approximated by this is an *overall* divergence, as it considers the posterior distribution of all datapoints as a whole, instead of averaging $D_{KL}(q_\phi(\mathbf{z}|\mathbf{x}) \| p_\theta(\mathbf{z}))$ across all datapoints as ELBo does.

On that basis, we can implement $\mathcal{L}_D(\boldsymbol{\theta}, \phi; \mathbf{x})$ with $D = D_{KL}$, which is equivalent to replacing the KL term in ELBo with $D_{KL}(q_\phi(\mathbf{z}) \| p_\theta(\mathbf{z}))$ approximated by Eq. 6. According to the decomposition (illustrated in Eq. 7) of the KL term in ELBo given by Hoffman et al. [19], maximizing $\mathcal{L}_{D_{KL}}(\boldsymbol{\theta}, \phi; x_n)$ on the whole dataset, $X = \{x_n\}_{n=1}^N$, $q_\phi(\mathbf{n}) \equiv \frac{1}{N}$, is equivalent to maximizing ELBo as well as $\mathbb{I}_{q_\phi(\mathbf{n}, \mathbf{z})}[\mathbf{n}, \mathbf{z}]$,² the mutual information of \mathbf{z} and \mathbf{n} in their joint distribution $q_\phi(\mathbf{n}, \mathbf{z})$, as illustrated in Eq. 8.

$$\frac{1}{N} \sum_{n=1}^N D_{KL}(q_\phi(\mathbf{z}|x_n) \| p_\theta(\mathbf{z})) = D_{KL}(q_\phi(\mathbf{z}) \| p_\theta(\mathbf{z})) + \mathbb{I}_{q_\phi(\mathbf{n}, \mathbf{z})}[\mathbf{n}, \mathbf{z}]$$

$$\text{where } \mathbb{I}_{q_\phi(\mathbf{n}, \mathbf{z})}[\mathbf{n}, \mathbf{z}] = \mathbb{E}_{q_\phi(\mathbf{n}, \mathbf{z})}[\log \frac{q_\phi(\mathbf{n}, \mathbf{z})}{q_\phi(\mathbf{n})q_\phi(\mathbf{z})}] \quad (7)$$

$$\text{where } q_\phi(\mathbf{n}, \mathbf{z}) = q_\phi(n)q_\phi(\mathbf{z}|n) = \frac{1}{N} q_\phi(\mathbf{z}|x_n)$$

¹Although we can have $q_\phi(z) = 0$, $z \in R^{Dim}$ when the latent variable follows a von Mises-Fisher (vMF) distribution, we do not need to consider such points in regularization.

²Posterior collapse (or KL vanishing) can be solved effectively by maximizing this mutual information term as it is a lower bound of the vanished KL divergence term in ELBo according to Eq. 7.

$$\begin{aligned}
\frac{1}{N} \sum_{n=1}^N [\mathcal{L}_{D_{KL}}(\boldsymbol{\theta}, \boldsymbol{\phi}; x_n)] &= \frac{1}{N} \sum_{n=1}^N [\mathbb{E}_{q_{\boldsymbol{\phi}}(\mathbf{z}|x_n)}[\log p_{\boldsymbol{\theta}}(x_n|\mathbf{z})]] - D_{KL}(q_{\boldsymbol{\phi}}(\mathbf{z})\|p_{\boldsymbol{\theta}}(\mathbf{z})) \\
&= \frac{1}{N} \sum_{n=1}^N [\mathcal{L}_{ELBo}(\boldsymbol{\theta}, \boldsymbol{\phi}; x_n)] + \mathbb{I}_{q_{\boldsymbol{\phi}}(\mathbf{n}, \mathbf{z})}[\mathbf{n}, \mathbf{z}]
\end{aligned} \tag{8}$$

Optimization on Mini-Batch Theoretically attractive as it is, maximizing $\mathcal{L}_{D_{KL}}(\boldsymbol{\theta}, \boldsymbol{\phi}; x_n)$ approximated by $DG(\boldsymbol{\theta}, \boldsymbol{\phi}; z_s)$ is undesirable for training VAEs on large datasets, because the probabilistic density of $q_{\boldsymbol{\phi}}(\mathbf{z})$ at z needs computation across the whole dataset and is changing in every training step. In practice, training deep networks such as VAEs commonly adopts mini-batch gradient descent, where only a small subset of the dataset is used for calculating gradients and updating parameters in each iteration step.

So, a practicable way is to aggregate the posterior of datapoints inside a mini-batch $B = \{x_n\}_{n=1}^{|B|}$, $q_{\boldsymbol{\phi}}(\mathbf{n}) \equiv \frac{1}{|B|}$, as stated in Eq. 9, where $z_{n,m}$ is the m^{th} sample from the posterior of datapoint x_n . Here, stratified sampling is used to ensure a steady Monte Carlo approximation,³ and the reparameterization trick [21] is applied to ensure a differentiable output.

$$\begin{aligned}
DG(\boldsymbol{\theta}, \boldsymbol{\phi}, B; z) &= \log \frac{q_{\boldsymbol{\phi}, B}(z)}{p_{\boldsymbol{\theta}}(z)} = \log \frac{\frac{1}{|B|} \sum_{n=1}^{|B|} q_{\boldsymbol{\phi}}(z|x_n)}{p_{\boldsymbol{\theta}}(z)} \\
D_{KL}(q_{\boldsymbol{\phi}, B}(\mathbf{z})\|p_{\boldsymbol{\theta}}(\mathbf{z})) &\approx \frac{1}{|B|} \sum_{n=1}^{|B|} \frac{1}{M} \sum_{m=1}^M DG(\boldsymbol{\theta}, \boldsymbol{\phi}, B; z_{n,m}), \text{ where } z_{n,m} \stackrel{idd}{\sim} q_{\boldsymbol{\phi}}(\mathbf{z}|x_n)
\end{aligned} \tag{9}$$

Through this approximation, we can implement $\mathcal{L}_{D_{KL}}(\boldsymbol{\theta}, \boldsymbol{\phi}, B; x_n)$ that regularizes $q_{\boldsymbol{\phi}, B}(\mathbf{z})$ towards $p_{\boldsymbol{\theta}}(\mathbf{z})$ for a mini-batch B , as stated in Eq. 10.

$$\begin{aligned}
\frac{1}{|B|} \sum_{n=1}^{|B|} [\mathcal{L}_{D_{KL}}(\boldsymbol{\theta}, \boldsymbol{\phi}, B; x_n)] &= \frac{1}{|B|} \sum_{n=1}^{|B|} [\mathbb{E}_{q_{\boldsymbol{\phi}}(\mathbf{z}|x_n)}[\log p_{\boldsymbol{\theta}}(x_n|\mathbf{z})]] - D_{KL}(q_{\boldsymbol{\phi}, B}(\mathbf{z})\|p_{\boldsymbol{\theta}}(\mathbf{z})) \\
&= \frac{1}{|B|} \sum_{n=1}^{|B|} [\mathcal{L}_{ELBo}(\boldsymbol{\theta}, \boldsymbol{\phi}; x_n)] + \mathbb{I}_{q_{\boldsymbol{\phi}}(\mathbf{n}, \mathbf{z})}[\mathbf{n}, \mathbf{z}]
\end{aligned} \tag{10}$$

It should be noticed that the mutual information term $\mathbb{I}_{q_{\boldsymbol{\phi}}(\mathbf{n}, \mathbf{z})}[\mathbf{n}, \mathbf{z}]$ is different in Eq. 8 (on the whole dataset) and Eq. 10 (on a mini-batch), because the range of discrete variable \mathbf{n} is from 1 to N in Eq. 8, but 1 to $|B|$ in Eq. 10. Consequently, $\mathbb{I}_{q_{\boldsymbol{\phi}}(\mathbf{n}, \mathbf{z})}[\mathbf{n}, \mathbf{z}]$ has an upper bound of $H(\mathbf{n}) = \log N$ in Eq. 8, but $H(\mathbf{n}) = \log |B|$ in Eq. 10. In other words, maximizing $\mathbb{I}_{q_{\boldsymbol{\phi}}(\mathbf{n}, \mathbf{z})}[\mathbf{n}, \mathbf{z}]$ in Eq. 8 intends to distinguish \mathbf{z} of x_n from that of $N - 1$ other datapoints, while it is limited to $|B| - 1$ other datapoints in Eq. 10.

Marginal Regularization for More Mutual Information As described above, approximating and optimizing $D_{KL}(q_{\boldsymbol{\phi}, B}(\mathbf{z})\|p_{\boldsymbol{\theta}}(\mathbf{z}))$ is practicable but has limited effect. Empirically, Gaussian distribution-based VAEs trained by Eq. 10 still have limited active units, which means the encoded latent variable \mathbf{z} still collapses to the prior on most dimensions, where it provides little information.

To activate \mathbf{z} on all dimensions, we propose to regularize $q_{\boldsymbol{\phi}, B}(\mathbf{z})$ towards $p_{\boldsymbol{\theta}}(\mathbf{z})$ on each dimension respectively, i.e., regularize the marginal distribution of $q_{\boldsymbol{\phi}, B}(\mathbf{z})$ on each dimension, as illustrated in Eq. 11, where $z_i \in R$ is the i^{th} component of $z \in R^{Dim}$ and the corresponding probability density functions are of the marginal distributions on the i^{th} dimension; and $z_{n,m,i}$ is the i^{th} component of

³In other words, we sample $S = |B| \times M$ samples from $q_{\boldsymbol{\phi}, B}(z)$ through sampling M samples from $q_{\boldsymbol{\phi}}(\mathbf{z}|x_n)$ for each datapoint $x_n \in B$.

the m^{th} sample from the posterior of datapoint x_n .

$$\begin{aligned}
DG_{mrg}(\boldsymbol{\theta}, \boldsymbol{\phi}, B; z_i) &= \log \frac{q_{\boldsymbol{\phi}, B}(z_i)}{p_{\boldsymbol{\theta}}(z_i)} = \log \frac{\frac{1}{|B|} \sum_{n=1}^{|B|} q_{\boldsymbol{\phi}}(z_i | x_n)}{p_{\boldsymbol{\theta}}(z_i)} \\
D_{KL, mrg}(q_{\boldsymbol{\phi}, B}(\mathbf{z}) \| p_{\boldsymbol{\theta}}(\mathbf{z})) &= \sum_{i=1}^{Dim} D_{KL}(q_{\boldsymbol{\phi}, B}(\mathbf{z}_i) \| p_{\boldsymbol{\theta}}(\mathbf{z}_i)) \\
&\approx \sum_{i=1}^{Dim} \frac{1}{|B|} \sum_{n=1}^{|B|} \frac{1}{M} \sum_{m=1}^M DG_{mrg}(\boldsymbol{\theta}, \boldsymbol{\phi}, B; z_{n,m,i})
\end{aligned} \tag{11}$$

In Gaussian distribution-based VAEs, the marginal distributions of \mathbf{z} on different dimensions are independent, i.e., $q_{\boldsymbol{\phi}}(\mathbf{z}|x_n) = \prod_i^{Dim} q_{\boldsymbol{\phi}}(\mathbf{z}_i|x_n)$ and $p_{\boldsymbol{\theta}}(\mathbf{z}) = \prod_i^{Dim} p_{\boldsymbol{\theta}}(\mathbf{z}_i)$, so their KL divergence can be decomposed as $D_{KL}(q_{\boldsymbol{\phi}}(\mathbf{z}|x_n) \| p_{\boldsymbol{\theta}}(\mathbf{z})) = \sum_i^{Dim} D_{KL}(q_{\boldsymbol{\phi}}(\mathbf{z}_i|x_n) \| p_{\boldsymbol{\theta}}(\mathbf{z}_i))$. Thus, we can infer the decomposition of $D_{KL, mrg}(q_{\boldsymbol{\phi}, B}(\mathbf{z}) \| p_{\boldsymbol{\theta}}(\mathbf{z}))$ through Eq. 12.

$$\begin{aligned}
D_{KL, mrg}(q_{\boldsymbol{\phi}, B}(\mathbf{z}) \| p_{\boldsymbol{\theta}}(\mathbf{z})) &= \sum_{i=1}^{Dim} D_{KL}(q_{\boldsymbol{\phi}, B}(\mathbf{z}_i) \| p_{\boldsymbol{\theta}}(\mathbf{z}_i)) \\
&= \sum_{i=1}^{Dim} \left[\frac{1}{|B|} \sum_n [D_{KL}(q_{\boldsymbol{\phi}}(\mathbf{z}_i|x_n) \| p_{\boldsymbol{\theta}}(\mathbf{z}_i))] - \mathbb{I}_{q_{\boldsymbol{\phi}}(\mathbf{n}, \mathbf{z}_i)}[\mathbf{n}, \mathbf{z}_i] \right] \\
&= \frac{1}{|B|} \sum_n [D_{KL}(q_{\boldsymbol{\phi}}(\mathbf{z}|x_n) \| p_{\boldsymbol{\theta}}(\mathbf{z}))] - \sum_{i=1}^{Dim} [\mathbb{I}_{q_{\boldsymbol{\phi}}(\mathbf{n}, \mathbf{z}_i)}[\mathbf{n}, \mathbf{z}_i]]
\end{aligned} \tag{12}$$

So, maximizing $\mathcal{L}_{D_{KL, mrg}}(\boldsymbol{\theta}, \boldsymbol{\phi}, B; x_n)$ derived from Eq. 11 is equivalent to maximizing ELBo as well as the mutual information of n and \mathbf{z}_i for each dimension i respectively, as stated in Eq. 13. In other words, it intends to distinguish \mathbf{z}_i of x_n from that of $|B| - 1$ other datapoints for each dimension i respectively. We refer to our models based on this Density Gap-based regularization as DG-VAEs.

$$\begin{aligned}
\frac{1}{|B|} \sum_{n=1}^{|B|} [\mathcal{L}_{D_{KL, mrg}}(\boldsymbol{\theta}, \boldsymbol{\phi}, B; x_n)] &= \frac{1}{|B|} \sum_{n=1}^{|B|} [\mathbb{E}_{q_{\boldsymbol{\phi}}(\mathbf{z}|x_n)}[\log p_{\boldsymbol{\theta}}(x_n|\mathbf{z})] - D_{KL, mrg}(q_{\boldsymbol{\phi}, B}(\mathbf{z}) \| p_{\boldsymbol{\theta}}(\mathbf{z}))] \\
&= \frac{1}{|B|} \sum_{n=1}^{|B|} [\mathcal{L}_{ELBo}(\boldsymbol{\theta}, \boldsymbol{\phi}; x_n)] + \sum_{i=1}^{Dim} [\mathbb{I}_{q_{\boldsymbol{\phi}}(\mathbf{n}, \mathbf{z}_i)}[\mathbf{n}, \mathbf{z}_i]]
\end{aligned} \tag{13}$$

Aggregation Size for Ablation As discussed above, the size of mini-batch $|B|$ sets an upper bound of the mutual information term $\mathbb{I}_{q_{\boldsymbol{\phi}}(\mathbf{n}, \mathbf{z})}[\mathbf{n}, \mathbf{z}]$ (or $\mathbb{I}_{q_{\boldsymbol{\phi}}(\mathbf{n}, \mathbf{z}_i)}[\mathbf{n}, \mathbf{z}_i]$). To validate this impact, we further extend DG-VAEs through dividing the mini-batch into non-overlapping subsets $B = \bigcup_{i=1}^C b_i$, s.t. $b_j \cap b_i = \emptyset$ iff $i \neq j$, calculating and optimizing the KL divergence over each subset, i.e., $\frac{1}{C} \sum_{i=1}^C \frac{1}{|b_i|} \sum_{j=1}^{|b_i|} [\mathcal{L}_{D_{KL, mrg}}(\boldsymbol{\theta}, \boldsymbol{\phi}, b_i; x_n)]$, where C denotes the number of subsets and $|b_i| = \frac{|B|}{C}$ is the size of those subsets, which we refer to as the *aggregation size* and denote as $|b|$ for simplification. It can be inferred that the DG-VAE with $|b| = 1$ is equivalent to the vanilla VAE trained by ELBo, except that it approximates the KL term through Monte Carlo instead of integration.

Extension to von Mises-Fisher Distribution-based VAEs Besides the commonly used Gaussian distribution-based VAEs, we also consider von Mises-Fisher (vMF) distribution-based VAEs. As the decomposition $q_{\boldsymbol{\phi}}(\mathbf{z}) = \prod_i^{Dim} q_{\boldsymbol{\phi}}(\mathbf{z}_i)$ is not established for latent variables following vMF distributions (i.e., $\mathbf{z} \sim vMF(\boldsymbol{\mu}, \kappa)$), marginal regularization for vMF-VAEs may be not interpretable, so we only implement Eq. 10 in vMF-VAEs. We refer to those extensions as DG-vMF-VAEs.

Table 1: Statistics of sentences in the datasets

Dataset	Train	Valid	Test	Vocab size	Length (avg \pm std)
Yelp	100,000	10,000	10,000	19997	98.01 \pm 48.86
Yahoo	100,000	10,000	10,000	20001	80.76 \pm 46.21
Short-Yelp	100,000	10,000	10,000	8411	10.96 \pm 3.60
SNLI	100,000	10,000	10,000	9990	11.73 \pm 4.33

4 Experiments

4.1 Experimental Setup

Datasets We consider four public available datasets commonly used for VAE-based language modeling tasks in our experiments: Yelp [42], Yahoo [42, 44], a downsampled version of Yelp [35] (we denote this as Short-Yelp), and a downsampled version of SNLI [5, 23]. The statistics of these datasets are illustrated in Table 1. It can be viewed that Yelp and Yahoo contain long sentences while Short-Yelp and SNLI contain short sentences.

Baselines We consider a wide range of VAEs for solving posterior collapse in text generation, where the hyperparameters are set according to Zhu et al. [46]:

- VAEs with modified training strategies (i.e., KL annealing): VAE with linear KL annealing in the first 10 epochs (default) [6]; VAE with linear KL annealing for 10 epochs at the start of every 20 epochs (cyclic-VAE) [13];
- VAEs with specific model structures: VAE with additional Bag-of-Words loss (bow-VAE) [45], and VAE with skip connection from the latent variable \mathbf{z} to the vocabulary classifier for generation (skip-VAE) [9];
- VAEs with hard restrictions on the posterior distribution: δ -VAE with the committed rate $\delta = 0.15$ [31]; BN-VAEs with the scale of BN layer $\gamma \in \{0.6, 0.7, 0.9, 1.2, 1.5, 1.8\}$ [46]; vMF-VAEs with the distribution’s concentration $\kappa \in \{13, 25, 50, 100, 200\}$ [8, 41];
- VAEs with weakened KL regularization: FB-VAEs (free-bits) with the target KL $\lambda_{KL} \in \{4, 9, 16, 25, 36, 49\}$ [20]; β -VAEs with the weight of the KL term in ELBo $\beta \in \{0.0, 0.1, 0.2, 0.4, 0.8\}$ [18].

Configurations We completely follow Zhu et al. [46] in the models’ backbone structures, data pre-processing, and training procedure, which we describe in detail in Appendix B.

4.2 Language Modeling

We evaluate the performance of our methods and the baselines on language modeling, where the following metrics are reported: the prior log likelihood $priorLL(\theta)$ and the posterior log likelihood $postLL(\theta, \phi)$ for generation quality; the KL term in ELBo $KL(\phi)$, the mutual information $MI(\phi)$ of \mathbf{z} and \mathbf{n} and the number of active units $AU(\phi)$ [7] for posterior collapse; and the number of consistent units $CU(\phi)$ (we propose) for the hole problem. The corresponding expressions and explanations are presented in Appendix C.

We illustrate part of the results on Yahoo in Table 2 and all results on all datasets in Appendix D. It can be observed that: (1) models with modified training strategies or specific model structures can alleviate the problem of posterior collapse but has limited effect according to $MI(\phi)$ and $AU(\phi)$; (2) models with hard restrictions or weakened KL regularization on the posterior can solve posterior collapse better through harder restrictions or further weakening according to the increase of $KL(\phi)$, $MI(\phi)$, and $AU(\phi)$, but the decrease of $CU(\phi)$ indicates that their posterior latent spaces tend to be increasingly inconsistent with that of the prior; (3) in contrast, our proposed DG-VAE has similar performance to the vanilla VAE when $|b| = 1$, and with the increase of $|b|$, it can solve posterior collapse effectively and avoid the hole problem at the same time.⁴

⁴There’s a little difference between DG-VAE ($|b| = 32$) and DG-VAE (default): DG-VAE ($|b| = 32$) ignores data batch B if $|B| < 32$ while DG-VAE (default) accepts it through adapting to its batch size.

Table 2: Results of Language Modeling on Yahoo dataset. We bold up $MI(\phi) \geq 9.0$, $AU(\phi) \geq 30$, $CU(\phi) \geq 30$, the highest $priorLL(\theta)$ and $postLL(\theta, \phi)$ for the same methods.

Models	$priorLL(\theta)$	$postLL(\theta, \phi)$	$KL(\phi)$	$MI(\phi)$	$AU(\phi)$	$CU(\phi)$
VAE (default)	-330.7	-330.7	0.0	0.0	0	32
cyclic-VAE	-329.8	-328.9	1.1	1.0	2	31
bow-VAE	-330.5	-330.5	0.0	0.0	0	32
skip-VAE	-330.1	-325.2	5.0	4.3	8	31
δ -VAE(0.15)	-330.5	-330.6	4.8	0.0	0	0
BN-VAE(0.6)	-327.6	-321.1	6.6	5.9	32	32
BN-VAE(1.2)	-330.9	-310.1	26.2	9.2	32	0
BN-VAE(1.8)	-343.5	-308.6	51.3	9.2	32	0
FB-VAE(4)	-329.8	-328.4	3.9	1.8	32	32
FB-VAE(16)	-325.7	-320.8	16.1	8.5	32	8
FB-VAE(49)	-344.6	-296.1	50.0	9.2	32	0
β -VAE(0.4)	-330.8	-324.8	7.0	6.7	3	31
β -VAE(0.2)	-338.6	-310.3	30.1	9.2	22	25
β -VAE(0.1)	-369.9	-289.6	83.7	9.2	32	0
DG-VAE ($ b = 1$)	-330.7	-330.7	0.0	0.0	0	32
DG-VAE ($ b = 4$)	-330.4	-318.3	14.3	9.1	11	32
DG-VAE ($ b = 32$)	-355.4	-294.1	65.2	9.1	32	32
DG-VAE (default)	-358.0	-290.8	70.8	9.1	32	32

It can also be viewed that with the increase of $MI(\phi)$ or $KL(\phi)$, $postLL(\theta, \phi)$ tends to increase, while $priorLL(\theta)$ tends to decrease, as the decoder θ becomes more dependent on the encoder ϕ . We further plot the curves of $priorLL(\theta)$ and $postLL(\theta, \phi)$ for models with different hyperparameters in Figure 2, where we can observe that DG-VAEs make better trade-offs than BN-VAEs and β -VAEs do on short datasets and perform competitively to BN-VAEs and FB-VAEs on long datasets.

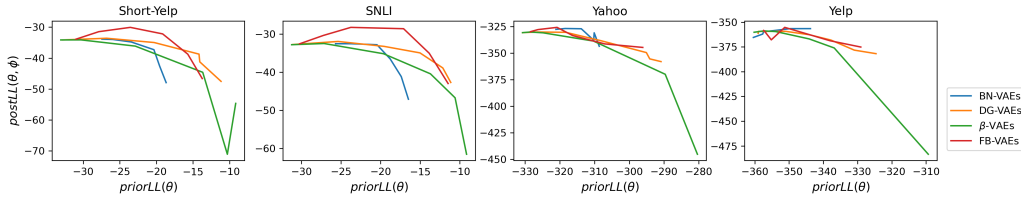


Figure 2: The curves of $priorLL(\theta)$ and $postLL(\theta, \phi)$ in Gaussian distribution-based VAEs.

We also compare the performance of DG-vMF-VAEs with vMF-VAEs under different settings of κ . As they have the same $KL(\phi)$, while $AU(\phi)$ and $CU(\phi)$ are inappropriate to report for vMF distributions, we only plot their curves of $priorLL(\theta)$ and $postLL(\theta, \phi)$ in Figure 3. It can be observed that DG-vMF-VAEs outperform vMF-VAEs in most cases.

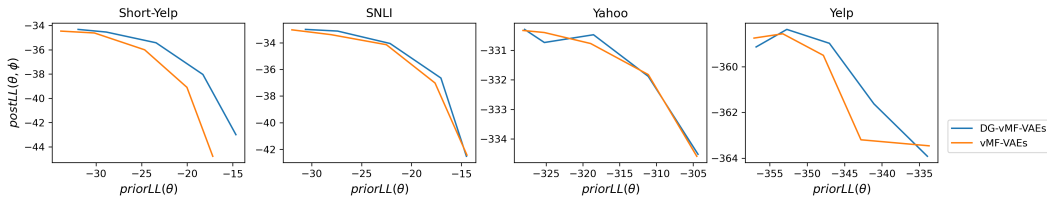


Figure 3: The curves of $priorLL(\theta)$ and $postLL(\theta, \phi)$ in vMF distribution-based VAEs.

4.3 Visualization of the Posterior

To further investigate the posterior distribution in latent space of those models, we visualize the aggregated posterior distributions and the posterior centers distributions on the 2 most active dimensions, i.e., the two dimensions with the highest $Var_{\mathbf{x} \sim \mathbf{X}}[\mathbb{E}_{q_\phi(\mathbf{z}|\mathbf{x})}[\mathbf{z}]]$, as depicted in Figure 4.

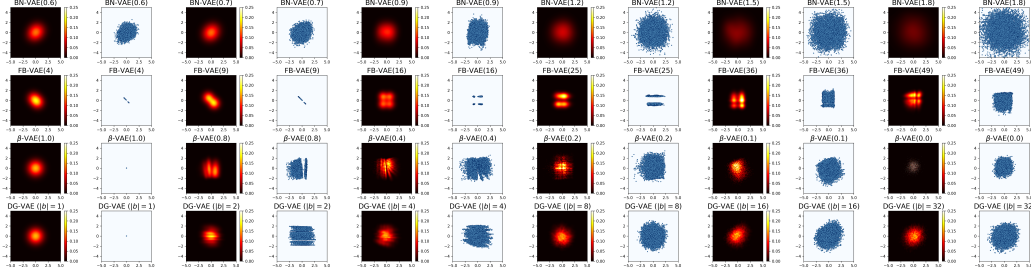


Figure 4: The visualization of the aggregated posterior distributions (red-in-black) and the posterior centers distributions (blue-in-white) for BN-VAEs, FB-VAEs, β -VAEs, and DG-VAEs on the Yahoo test-set. Illustrations for more datasets, more models, and more dimensions, are shown in Appendix G.

Here, we can observe that BN-VAEs, FB-VAEs and β -VAEs can better solve posterior collapse with harder restrictions or further weakening, but meanwhile they are faced with different kinds of mismatch between the aggregated posterior distribution and the prior distribution, i.e., the hole problem. In contrast, with the increase of aggregation size $|b|$, DG-VAE can better solve posterior collapse and avoid the hole problem in the meantime.

4.4 Interpolation Study

One of the main advantages of VAEs over normal language models (e.g., GPT-2 [30]) is that VAEs embed datapoints into a continuous latent space and thus enable latent-guided generation. We evaluate this ability through interpolation, where the models encode two sentences \mathbf{x}_a and \mathbf{x}_b as their posterior centers, i.e., $z_a = \mathbb{E}_{q_\phi(\mathbf{z}|\mathbf{x}_a)}[\mathbf{z}]$ and $z_b = \mathbb{E}_{q_\phi(\mathbf{z}|\mathbf{x}_b)}[\mathbf{z}]$, and decode the variables between them, i.e., $z_\lambda = z_a \cdot (1 - \lambda) + z_b \cdot \lambda$, $\lambda \in \{0.0, 0.1, \dots, 1.0\}$.⁵ The interpolated sentences are wished to be semantically smooth and meaningful, which we evaluate through the average Rouge-L F1-score [26], as stated in Eq. 14, where F_{lcs} denotes the F1-score of Longest Common Subsequence (LCS). We plot the curves of Rouge-L F1-score and λ for models on Yahoo dataset in Figure 5 and those curves on other datasets in Appendix E.

$$RougeLF1(\mathbf{x}_a, \mathbf{x}_b, \mathbf{x}_\lambda) = \frac{1}{2}(F_{lcs}(\mathbf{x}_a, \mathbf{x}_\lambda) + F_{lcs}(\mathbf{x}_b, \mathbf{x}_\lambda)) \quad (14)$$

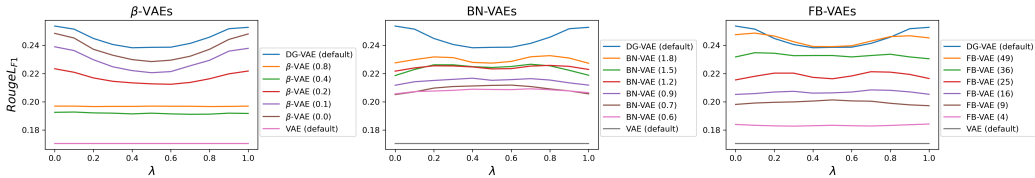


Figure 5: The curves of Rouge-L F1-score and λ for models' interpolation performance on Yahoo.

As shown in Figure 5, the average F1-score of LCS tends to be lower in the middle than at the ends, which indicates that generated sentences tend to not be smooth in the middle, which corresponds to the phenomenon of generation near to holes observed in previous work [25]⁶. The vanilla VAE performs the worst as it suffers from posterior collapse, and only generates the same plain sentence;

⁵We only consider greedy search for generation in this work.

⁶For further illustration on this phenomenon, we provide case study in Appendix F.

meanwhile, DG-VAE outperforms BN-VAEs, FB-VAEs and β -VAEs in the quality of interpolation on the Yahoo dataset as it can solve posterior collapse and avoid the hole problem at the same time.

In summary, the existing methods for solving posterior collapse in VAEs either have limited effect or can effectively solve posterior collapse at the cost of bringing the hole problem. In contrast, our proposed DG-VAE can effectively solve posterior collapse and avoid the hole problem at the same time, which is demonstrated by the posterior centers spread in latent space and the aggregated posterior distribution consistent with the prior distribution. Furthermore, our proposed DG-VAE outperforms the existing methods in the quality of latent-guided generation due to these improvements in latent space.

5 Discussion

Conclusion In this work, we perform systematic experiments to demonstrate posterior collapse and the hole problem in existing continuous VAEs for text generation. To solve both problems at the same time, we propose a density gap-based regularization on the aggregated posterior distribution to replace the KL regularization in ELBo, and prove it in essence maximizes the ELBo as well as the mutual information between the latent and the input. Experiments on real-world datasets prove the effectiveness of our method in solving both problems and its improvement in latent-guided generation.

Limitation & Future work Both the theory and the ablation study show that the effectiveness of our proposed method depends on the aggregation size $|b|$, which is still limited by the batch size during training. Therefore a promising future direction is to find a solution to break this limit, such like the memory bank mechanism in contrastive learning [38].

Acknowledgments and Disclosure of Funding

This work was supported in part by the State Key Laboratory of the Software Development Environment of China under Grant SKLSDE-2021ZX-16.

References

- [1] Jyoti Aneja, Alexander G. Schwing, Jan Kautz, and Arash Vahdat. A contrastive learning approach for training variational autoencoder priors. In *Proceedings of the 2021 Annual Conference on Neural Information Processing Systems*, pages 480–493, 2021.
- [2] Hareesh Bahuleyan, Lili Mou, Hao Zhou, and Olga Vechtomova. Stochastic Wasserstein autoencoder for probabilistic sentence generation. In *Proceedings of the 2019 Conference of the North American Chapter of the Association for Computational Linguistics: Human Language Technologies*, pages 4068–4076, 2019.
- [3] Matthias Bauer and Andriy Mnih. Resampled priors for variational autoencoders. In *Proceedings of the 22nd International Conference on Artificial Intelligence and Statistics*, pages 66–75, 2019.
- [4] Sam Bond-Taylor, Adam Leach, Yang Long, and Chris G. Willcocks. Deep generative modelling: A comparative review of VAEs, GANs, normalizing flows, energy-based and autoregressive models. *CoRR*, abs/2103.04922, 2021.
- [5] Samuel R. Bowman, Gabor Angeli, Christopher Potts, and Christopher D. Manning. A large annotated corpus for learning natural language inference. In *Proceedings of the 2015 Conference on Empirical Methods in Natural Language Processing*, pages 632–642, 2015.
- [6] Samuel R. Bowman, Luke Vilnis, Oriol Vinyals, Andrew M. Dai, Rafal Józefowicz, and Samy Bengio. Generating sentences from a continuous space. In *Proceedings of the 20th SIGNLL Conference on Computational Natural Language Learning*, pages 10–21, 2016.
- [7] Yuri Burda, Roger B. Grosse, and Ruslan Salakhutdinov. Importance weighted autoencoders. In *Proceedings of the 4th International Conference on Learning Representations*, 2016.

- [8] Tim R. Davidson, Luca Falorsi, Nicola De Cao, Thomas Kipf, and Jakub M. Tomczak. Hyper-spherical variational auto-encoders. In *Proceedings of the 34th Conference on Uncertainty in Artificial Intelligence*, pages 856–865, 2018.
- [9] Adji B. Dieng, Yoon Kim, Alexander M. Rush, and David M. Blei. Avoiding latent variable collapse with generative skip models. In *Proceedings of the 22nd International Conference on Artificial Intelligence and Statistics*, pages 2397–2405, 2019.
- [10] Yue Ding, Yuxiang Shi, Bo Chen, Chenghua Lin, Hongtao Lu, Jie Li, Ruiming Tang, and Dong Wang. Semi-deterministic and contrastive variational graph autoencoder for recommendation. In *Proceedings of the 30th ACM International Conference on Information and Knowledge Management*, pages 382–391, 2021.
- [11] Le Fang, Chunyuan Li, Jianfeng Gao, Wen Dong, and Changyou Chen. Implicit deep latent variable models for text generation. In *Proceedings of the 2019 Conference on Empirical Methods in Natural Language Processing and the 9th International Joint Conference on Natural Language Processing*, pages 3944–3954, 2019.
- [12] Qingkai Fang and Yang Feng. Neural machine translation with phrase-level universal visual representations. In *Proceedings of the 60th Annual Meeting of the Association for Computational Linguistics*, pages 5687–5698, 2022.
- [13] Hao Fu, Chunyuan Li, Xiaodong Liu, Jianfeng Gao, Asli Celikyilmaz, and Lawrence Carin. Cyclical annealing schedule: A simple approach to mitigating KL vanishing. In *Proceedings of the 2019 Conference of the North American Chapter of the Association for Computational Linguistics: Human Language Technologies*, pages 240–250, 2019.
- [14] Tingchen Fu, Xueliang Zhao, Chongyang Tao, Ji-Rong Wen, and Rui Yan. There are a thousand hamlets in a thousand people’s eyes: Enhancing knowledge-grounded dialogue with personal memory. In *Proceedings of the 60th Annual Meeting of the Association for Computational Linguistics*, pages 3901–3913, 2022.
- [15] Ian J. Goodfellow, Jean Pouget-Abadie, Mehdi Mirza, Bing Xu, David Warde-Farley, Sherjil Ozair, Aaron C. Courville, and Yoshua Bengio. Generative adversarial nets. In *Proceedings of 2014 Annual Conference on Neural Information Processing Systems*, pages 2672–2680, 2014.
- [16] Ishaan Gulrajani, Kundan Kumar, Faruk Ahmed, Adrien Ali Taïga, Francesco Visin, David Vázquez, and Aaron C. Courville. PixelVAE: A latent variable model for natural images. In *Proceedings of the 5th International Conference on Learning Representations*, 2017.
- [17] Serhii Havrylov and Ivan Titov. Preventing posterior collapse with levenshtein variational autoencoder. *CoRR*, abs/2004.14758, 2020.
- [18] Irina Higgins, Loïc Matthey, Arka Pal, Christopher Burgess, Xavier Glorot, Matthew Botvinick, Shakir Mohamed, and Alexander Lerchner. beta-VAE: Learning basic visual concepts with a constrained variational framework. In *Proceedings of the 5th International Conference on Learning Representations*, 2017.
- [19] Matthew D Hoffman and Matthew J Johnson. ELBO surgery: Yet another way to carve up the variational evidence lower bound. In *Proceedings of 2016 NIPS Workshop on Advances in Approximate Bayesian Inference*, 2016.
- [20] Diederik P. Kingma, Tim Salimans, Rafal Józefowicz, Xi Chen, Ilya Sutskever, and Max Welling. Improving variational autoencoders with inverse autoregressive flow. In *Proceedings of the 2016 Annual Conference on Neural Information Processing Systems*, pages 4736–4744, 2016.
- [21] Diederik P. Kingma and Max Welling. Auto-encoding variational Bayes. In *Proceedings of the 2nd International Conference on Learning Representations*, 2014.
- [22] Alexej Klushyn, Nutan Chen, Richard Kurle, Botond Cseke, and Patrick van der Smagt. Learning hierarchical priors in VAEs. In *Proceedings of the 2019 Annual Conference on Neural Information Processing Systems*, pages 2866–2875, 2019.

- [23] Bohan Li, Junxian He, Graham Neubig, Taylor Berg-Kirkpatrick, and Yiming Yang. A surprisingly effective fix for deep latent variable modeling of text. In *Proceedings of the 2019 Conference on Empirical Methods in Natural Language Processing and the 9th International Joint Conference on Natural Language Processing*, pages 3601–3612, 2019.
- [24] Ruizhe Li, Xiao Li, Guanyi Chen, and Chenghua Lin. Improving variational autoencoder for text modelling with timestep-wise regularisation. In *Proceedings of the 28th International Conference on Computational Linguistics*, pages 2381–2397, 2020.
- [25] Ruizhe Li, Xutan Peng, and Chenghua Lin. On the latent holes of VAEs for text generation. *CoRR*, abs/2110.03318, 2021.
- [26] Chin-Yew Lin. ROUGE: A package for automatic evaluation of summaries. In *Proceedings of 2004 Text Summarization Branches Out*, 2004.
- [27] Micha Livne, Kevin Swersky, and David J. Fleet. SentenceMIM: A latent variable language model. *CoRR*, abs/2003.02645, 2020.
- [28] Alireza Makhzani, Jonathon Shlens, Navdeep Jaitly, and Ian J. Goodfellow. Adversarial autoencoders. *CoRR*, abs/1511.05644, 2015.
- [29] Alban Petit and Caio Corro. Preventing posterior collapse in variational autoencoders for text generation via decoder regularization. *CoRR*, abs/2110.14945, 2021.
- [30] Alec Radford, Jeffrey Wu, Rewon Child, David Luan, Dario Amodei, Ilya Sutskever, et al. Language models are unsupervised multitask learners. *OpenAI blog*, 1(8):9, 2019.
- [31] Ali Razavi, Aäron van den Oord, Ben Poole, and Oriol Vinyals. Preventing posterior collapse with delta-VAEs. In *Proceedings of the 7th International Conference on Learning Representations*, 2019.
- [32] Danilo Jimenez Rezende, Shakir Mohamed, and Daan Wierstra. Stochastic backpropagation and approximate inference in deep generative models. In *Proceedings of the 31th International Conference on Machine Learning*, pages 1278–1286, 2014.
- [33] Danilo Jimenez Rezende and Fabio Viola. Taming VAEs. *CoRR*, abs/1810.00597, 2018.
- [34] Harshil Shah and David Barber. Generative neural machine translation. In *Proceedings of the 2018 Annual Conference on Neural Information Processing Systems*, pages 1353–1362, 2018.
- [35] Tianxiao Shen, Tao Lei, Regina Barzilay, and Tommi S. Jaakkola. Style transfer from non-parallel text by cross-alignment. In *Proceedings of the 2017 Annual Conference on Neural Information Processing Systems*, pages 6830–6841, 2017.
- [36] Ilya O. Tolstikhin, Olivier Bousquet, Sylvain Gelly, and Bernhard Schölkopf. Wasserstein auto-encoders. In *Proceedings of the 6th International Conference on Learning Representations*, 2018.
- [37] Jakub M. Tomczak and Max Welling. VAE with a vampprior. In *Proceedings of the 21st International Conference on Artificial Intelligence and Statistics*, pages 1214–1223, 2018.
- [38] Zhirong Wu, Yuanjun Xiong, Stella X. Yu, and Dahua Lin. Unsupervised feature learning via non-parametric instance discrimination. In *Proceedings of the 2018 IEEE Conference on Computer Vision and Pattern Recognition*, pages 3733–3742, 2018.
- [39] Congying Xia, Caiming Xiong, and Philip S. Yu. Pseudo siamese network for few-shot intent generation. In *Proceedings of the 44th International ACM SIGIR Conference on Research and Development in Information Retrieval*, pages 2005–2009, 2021.
- [40] Haowen Xu, Wenxiao Chen, Jinlin Lai, Zhihan Li, Youjian Zhao, and Dan Pei. On the necessity and effectiveness of learning the prior of variational auto-encoder. *CoRR*, abs/1905.13452, 2019.

- [41] Jiacheng Xu and Greg Durrett. Spherical latent spaces for stable variational autoencoders. In *Proceedings of the 2018 Conference on Empirical Methods in Natural Language Processing*, pages 4503–4513, 2018.
- [42] Zichao Yang, Zhiting Hu, Ruslan Salakhutdinov, and Taylor Berg-Kirkpatrick. Improved variational autoencoders for text modeling using dilated convolutions. In *Proceedings of the 34th International Conference on Machine Learning*, pages 3881–3890, 2017.
- [43] Kang Min Yoo, Youhyun Shin, and Sang-goo Lee. Data augmentation for spoken language understanding via joint variational generation. In *Proceedings of the 33rd AAAI Conference on Artificial Intelligence*, pages 7402–7409, 2019.
- [44] Xiang Zhang, Junbo Jake Zhao, and Yann LeCun. Character-level convolutional networks for text classification. In *Proceedings of the 2015 Annual Conference on Neural Information Processing Systems*, pages 649–657, 2015.
- [45] Tiancheng Zhao, Ran Zhao, and Maxine Eskénazi. Learning discourse-level diversity for neural dialog models using conditional variational autoencoders. In *Proceedings of the 55th Annual Meeting of the Association for Computational Linguistics*, pages 654–664, 2017.
- [46] Qile Zhu, Wei Bi, Xiaojiang Liu, Xiyao Ma, Xiaolin Li, and Dapeng Wu. A batch normalized inference network keeps the KL vanishing away. In *Proceedings of the 58th Annual Meeting of the Association for Computational Linguistics*, pages 2636–2649, 2020.

Checklist

1. For all authors...
 - (a) Do the main claims made in the abstract and introduction accurately reflect the paper’s contributions and scope? **[Yes]** We propose a novel regularization for VAEs to solve both posterior collapse and the hole problem.
 - (b) Did you describe the limitations of your work? **[Yes]** See Section 5.
 - (c) Did you discuss any potential negative societal impacts of your work? **[No]**
 - (d) Have you read the ethics review guidelines and ensured that your paper conforms to them? **[Yes]**
2. If you are including theoretical results...
 - (a) Did you state the full set of assumptions of all theoretical results? **[Yes]** We state the full set of assumptions in the first paragraph of Section 3.
 - (b) Did you include complete proofs of all theoretical results? **[Yes]** We provide complete proofs for all theoretical results in Section 3.
3. If you ran experiments...
 - (a) Did you include the code, data, and instructions needed to reproduce the main experimental results (either in the supplemental material or as a URL)? **[Yes]** We include the code, scripts for downloading data and instructions for reproduction in the supplemental material.
 - (b) Did you specify all the training details (e.g., data splits, hyperparameters, how they were chosen)? **[Yes]** See Appendix B.
 - (c) Did you report error bars (e.g., with respect to the random seed after running experiments multiple times)? **[No]**
 - (d) Did you include the total amount of compute and the type of resources used (e.g., type of GPUs, internal cluster, or cloud provider)? **[Yes]** See Appendix B.
4. If you are using existing assets (e.g., code, data, models) or curating/releasing new assets...
 - (a) If your work uses existing assets, did you cite the creators? **[Yes]** See Section 4.
 - (b) Did you mention the license of the assets? **[No]**
 - (c) Did you include any new assets either in the supplemental material or as a URL? **[No]**
 - (d) Did you discuss whether and how consent was obtained from people whose data you’re using/curating? **[N/A]**

- (e) Did you discuss whether the data you are using/curating contains personally identifiable information or offensive content? [No]
5. If you used crowdsourcing or conducted research with human subjects...
- (a) Did you include the full text of instructions given to participants and screenshots, if applicable? [N/A]
 - (b) Did you describe any potential participant risks, with links to Institutional Review Board (IRB) approvals, if applicable? [N/A]
 - (c) Did you include the estimated hourly wage paid to participants and the total amount spent on participant compensation? [N/A]